J|A|C|S
ARTICLES
Published on Web 10/23/2002

Cascade of Coil-Globule Conformational Transitions of Single Flexible Polyelectrolyte Molecules in Poor Solvent

Anton Kiriy,[†] Ganna Gorodyska,[†] Sergiy Minko,*[,†] Werner Jaeger,[‡] Petr Štěpánek,[§] and Manfred Stamm[†]

Contribution from the Institut für Polymerforschung Dresden, Hohe Strasse 6, 01069 Dresden, Germany, Department of Water Born Polymers, Fraunhofer-Institut für Angewandte Polymerforschung, Geiselbergstrasse 69, 14476 Golm, Germany, and Institute of Macromolecular Chemistry, Heyrovsky Sq. 2, 162 06 Praha 6 − Brevnov, Czech Republic

Received March 6, 2002

Abstract: We show that hydrophobic flexible polyelectrolyte molecules of poly(2-vinylpyridine) and poly(methacryloyloxyethyl dimethylbenzylammonium chloride) are trapped and frozen due to adsorption on the mica surface, and the observed AFM single molecule structures reflect the molecular conformation in solution. An increase of the ionic strength of the solution induces the cascade of abrupt conformational transitions due to the intrachain segregation from elongated coil to compact globule conformations through intermediate pearl necklace-globule conformations with different amounts of beads per chain. The length of the necklaces and the number of beads decrease, while the diameter of beads increases with the increase of ionic strength. Coexistence at the same time of extended coils, necklaces with different amounts of beads, and compact globules indicates the cascade of the first-order-type phase transitions.

Introduction

Polyelectrolytes (PE) are macromolecules with ionizable groups which dissociate in polar (aqueous) medium into polyions and counterions with opposite charges. An increase of entropy due to the release of counterions causes solubility of PE even with a hydrophobic backbone. PE macromolecules undergo diverse conformational transitions responding to change of environment (ionic strength, pH, condensation agents, temperature, concentration) driven by interplay between attractive short-range van der Waals and repulsive long-range Coulomb interactions. It is well known that at a high charge density PE chains display an extended coil conformation due to the electrostatic repulsion between charged monomer units. Decrease of the charge density results in a collapse transition of PE chains to a globule conformation due to the short-range interactions. A change of PE conformations in a controlled environment and, particularly, coil-to-globule transition (CGT) phenomena attract continuously enhanced interest due to their importance in industry and nature.[1] For example, gelation of PE in water and reversible swelling or shrinking of PE gels responding to external stimuli are considered to be the most promising properties of PE[2] on the basis of CGT phenomenon. Metallization of PE molecules in a controlled environment allows one to fabricate nanoparticles of the dedicated shape on the level of single molecules.[3]

CGT is considered to be a complicated process when the transition character depends on chain stiffness and specific interactions in the system.[4] Traditionally, polymer science considers CGT for flexible polymer chains as a gradual process which is associated with the second-order phase transition[5] (Figure 1a), while for stiff polymers the theory suggests[5,6] the sharp first-order phase transition (Figure 1c). In contrast to the theoretical predictions, many experimental results have indicated continuous character of CGT for different flexible and stiff polymer chains.[7] Single molecule experiments with stiff DNA molecules[8] and brush molecules[9] have shown that an individual chain exhibits a first-order phase transition between an elongated coil and a spherical or *ordered* toroidal[10] globule, while this transition appears continuous in the ensemble.

In contrast, DNA modified by synthetic polymers undergoes a continuous second-order phase transition through the set of partially collapsed *disordered* intrasegregated conformations.[11]

* To whom correspondence should be addressed. E-mail: minko@ipfdd.de. Tel: +49-351-4658-271. Fax: +49-351-4658-284.
[†] Institut für Polymerforschung Dresden.
[‡] Fraunhofer-Institut für Angewandte Polymerforschung.
[§] Institute of Macromolecular Chemistry.

(1) *Polyelectrolytes*; Hara, M., Ed.; Marcel Dekker: New York, 1993. Dautzenberg, H.; Jaeger, W.; Kötz, B. P. J.; Seidel, C.; Stscherbina, D. *Polyelectroytes: Formation, Characterization, and Application*; Hanser Publishers: Munich, Vienna, New York, 1994. Barrat, J.-L.; Joanny, J.-F. *Adv. Chem. Phys.* **1995**, *94*, 1. Förster, S.; Schmidt, M. *Adv. Polym. Sci.* **1995**, *120*, 51.
(2) Tanaka, T. *Phys. Rev. Lett.* **1978**, *40*, 820−823.
(3) Kiriy, A.; Minko, S.; Gorodyska, A.; Stamm, M.; Jaeger, W. *Nano Lett.* **2002**, *2*, 881−885. Minko, S.; Kiriy, A.; Gorodyska, G.; Stamm, M. *J. Am. Chem. Soc.* **2002**, *124*, 10192−10197.
(4) Lifshitz, I. M.; Grosberg, A. Yu.; Khokhlov, A. R. *Rev. Mod. Phys.* **1978**, *50*, 683−713.
(5) de Gennes, P. G. *Scaling Concepts in Polymer Physics*; Cornell University Press: New York, 1979.
(6) Vasilevskaya, V.; Khokhlov, A. R.; Matsuzawa, Y.; Yoshikawa, K. *J. Chem. Phys.* **1995**, *102*, 6595−6602. Vasilevskaya, V.; Khokhlov, A. R.; Kidoaki, S.; Yoshikawa, K. *Biopolymers* **1997**, *41*, 51−59. Kuznetsov, Y. A.; Timoshenko, E. G. *J. Chem. Phys.* **1999**, *111*, 3744−3752.
(7) For example: Cosule, L. C.; Schellman, J. A. *Nature* **1976**, *259*, 333. Widom, J.; Baldwin, R. L. *J. Mol. Biol.* **1980**, *144*, 431. Post, C. B.; Zimm, B. H. *Biopolymers* **1982**, *21*, 2123. Park, I. H.; Wang, Q. W.; Chu, B. *Macromolecules* **1987**, *20*, 1965−1969.

10.1021/ja0261168 CCC: $22.00

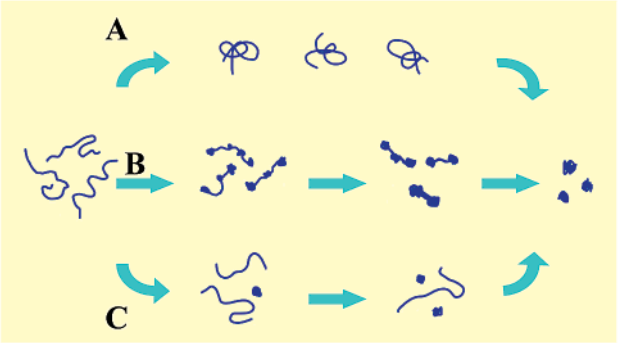

Figure 1. Outline of different CGT mechanisms for PE in poor solvent: continuous second-order phase transition (a); cascade of first-order transitions between necklaces, assumed for flexible PE (b); abrupt two-state first-order transition, found for stiff PE (c).

That displays the general tendency for polymers when highly cooperative all-or-non character of collapse transitions usually is realized for ordered folding reactions[12] or very stiff molecules,[6] if in both cases the density of the compact state is much larger than the density of the coil.[13] The mechanism of CGT for synthetic flexible PE on the single molecule level is still intensively discussed.

CGT for PE has a specific character due to the additional free energy component introduced by the Coulomb interaction, which, first of all, causes the influence of charge density on the conformations of the PE coil and globule. This effect is much more pronounced in the case of flexible PE as compared to stiff DNA molecules characterized with intrinsic stiffness introduced by intramolecular hydrogen bonds. Electrostatic repulsion affects elongated conformations of PE coils. Khokhlov has proposed a cylindrical conformation for the deformed weakly charged flexible PE globule in poor solvent.[14] Recent theoretical analysis predicts intermediate necklacelike conformations of weakly charged flexible PE chains (DRO model), when the chains adopt conformations resembling a sequence of polymer beads interconnected by narrow strings.[15] The theory suggests that a decrease of the charge density leads to a cascade of abrupt transitions between necklaces with different numbers of beads. Consequently, such a transition is an alternative to a continuous transition pass from coil to globule conformation of PE molecules and may be considered as a sequence of intrinsic first-order transitions between necklaces (Figure 1b). There are several experimental reports confirming these theoretical predictions.[16] However, it has been difficult to obtain fully conclusive results about the mechanism of CGT in a single PE chain, because the competition between single-chain events and an aggregation of several chains was always present under experimental conditions. In addition, conventional methods, such as laser light and neutron scattering, NMR spectroscopy, sedimentation, and conductivity, provide information referring to the ensemble average over many polymer chains. In the case of the highly fluctuating necklace conformations, one may assume that scattering experiments show an averaged picture of CGT. In this case, single molecule experiments are a powerful tool to clarify the mechanism of CGT via direct visualization of morphology of single molecules.

Recently, we reported on the direct observation of different conformations of single flexible poly(2-vinylpyridine) (P2VP) molecules adsorbed onto the flat surface.[17] It has been shown that P2VP molecules undergo stepwise conformational transitions from the stretched wormlike coil to compact globule via an intermediate necklacelike globule structure. This result addresses many questions whether we observe conformations corresponding to those in solution, or to the equilibrium adsorbed state, or whether they are formed under the strong influence of the sample preparation procedure, that is, drying of the sample.

In this paper, on the basis of both AFM and dynamic light-scattering (DLS) investigations, we report the further advance in the study of necklacelike conformations. In this study, besides P2VP we used the relatively "large" PE molecules of poly(methacryloyloxyethyl dimethylbenzylammonium chloride) (PMB):

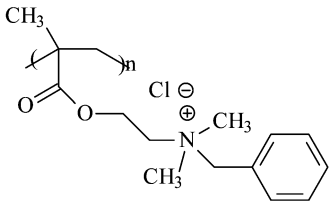

which allowed us to obtain much better resolution for AFM investigations as compared to P2VP and to identify some particular details of deposited-on-mica necklace structures in the dry state as well as under salt aqueous solution. In this report, we show that the addition of salt affects the PE globule conformation in the same fashion as a decrease of charge density. We present the direct evidence of the stepwise transitions between different necklace globules with the increased screening of electrostatic interactions and the ion condensation effect[15c,d] induced by addition of mono- and three-valence ions.

Experimental Section

Materials. Methacryloyloxyethyl dimethylbenzylammonium chloride (MB-Cl) from ATOCHEM and water-soluble initiator 2,2′-azobis (2-

(8) Yoshikawa, K.; Takahashi, M.; Vasilevskaya, V.; Khokhlov, A. R. *Phys. Rev. Lett.* **1996**, *76*, 3029−3031. Vasilevskaya, V.; Khokhlov, A. R.; Matsuzawa, Y.; Yoshikawa, K. *J. Chem. Phys.* **1996**, *102*, 6595−6602. Takahashi, M.; Yoshikawa, K.; Vasilevskaya, V.; Khokhlov, A. R. *J. Phys. Chem. B* **1997**, *101*, 9396−9401. Starodubtsev, S. G.; Yoshikawa, K. *Langmuir* **1998**, *14*, 214−217. Sergeev, V.; Mikhailenko, S.; Pyshkina, O.; Vaminsky, I.; Yoshikawa, K. *J. Am. Chem. Soc.* **1999**, *121*, 1780−1785. Iwataki, T.; Yoshikawa, K.; Kidoaki, S.; Umeno, D.; Kiji, M.; Maeda, M. *J. Am. Chem. Soc.* **2000**, *122*, 9891−9896.
(9) Sheiko, S. S.; Prokhorova, S. A.; Beers, K. L.; Matyjaszewski, K.; Potemkin, I. I.; Khokhlov, A. R.; Möller, M. *Macromolecules* **2001**, *34*, 8354−8360.
(10) Yoshikawa, Y.; Yoshikawa, K.; Kanbe, T. *Langmuir* **1999**, *15*, 5, 4085−4088. Ono, M. Y.; Spain, M. *J. Am. Chem. Soc.* **1997**, *119*, 77330-7334.
(11) Yoshikawa, K.; Yoshikawa, Y.; Koyama, Y.; Kanbe, T. *J. Am. Chem. Soc.* **1997**, *119*, 6473−6477. Starodubtsev, S. G.; Yoshikawa, K. *J. Phys. Chem.* **1996**, *100*, 19702−19705.
(12) Hill, D. J.; Mio, M. J.; Prince, R. B.; Hughes, T. S.; Moore, J. S. *Chem. Rev.* **2001**, *101*, 3893−4011.
(13) Grosberg, A. Yu.; Khokhlov, A. R. *Statistical Physics of Macromolecules*; AIP Press: New York, 1994.
(14) Khokhlov, A. R. *J. Phys. A* **1980**, *13*, 979−987.
(15) (a) Kantor, Y.; Kardar, M. *Phys. Rev. E* **1995**, *51*, 1299. (b) Dobrynin, A. V.; Rubinstein, M.; Obukhov, S. P. *Macromolecules* **1996**, *29*, 2974−2979. (c) Dobrynin, A. V.; Rubinstein, M. *Macromolecules* **1999**, *32*, 915−922. (d) Dobrynin, A. V.; Rubinstein, M. *Macromolecules* **2001**, *34*, 1964−1972. (e) Dobrynin, A. V.; Rubinstein, M. *Macromolecules* **2002**, *35*, 2754−2768. (f) Solis, F. J.; de la Cruz, M. O. *Macromolecules* **1998**, *31*, 5502−5506. (g) Lyulin, A. V.; Dünweg, B.; Borisov, O. V.; Darinskii, A. A. *Macromolecules* **1999**, *32*, 3264−3278. (h) Mica, U.; Holm, C.; Kremer, K. *Langmuir* **1999**, *15*, 4033−4044.
(16) Aseyev, V. O.; Klenin, S.; Tenhu, H.; Grillo, I.; Geissler, E. *Macromolecules* **2001**, *34*, 3706−3709. Wang, X.; Qiu, X.; Wu, C. *Macromolecules* **1998**, *31*, 2972−2976. Lee, M.-J.; Green, M. M.; Morawetz, H. *Macromolecules* **2002**, *35*, 4216−4217.
(17) Minko, S.; Kiriy, A.; Gorodyska, G.; Stamm, M. *J. Am. Chem. Soc.* **2002**, *124*, 3218−3219.

amidinepropane) hydrochloride (AAP) from WAKO were used without further purification. Synthesis and methods of PMB characterization were described elsewhere.[18] Polymerization of MB-Cl was carried out in aqueous solution using AAP as a cationic water-soluble initiator in a stirred tank reactor. The monomer solution was purged with nitrogen for 16 h at room temperature and then thermostated at reaction temperature. Polymerizations were run after injection of the solution of initiator in oxygen-free water under nitrogen at a reaction temperature of ±0.5 K. Further experimental conditions for the synthesis of polymers with different molecular weight are derived from kinetic data of the polymerization process.[18] To exclude side reactions and to follow the kinetics precisely, the polymerization was stopped at law conversion (10%) by rapid cooling and dilution in water. The polymers were purified by ultrafiltration (Minisette, Pall-Filtron, cut off 10 000 Dalton) and isolated by freeze-drying (Christ Beta 1/16).

For our study, we used two samples of PMB with different molecular weights: PMB-1 with $M_n = 480$ kg/mol, $M_w = 720$ kg/mol, $M_w/M_n = 1.5$, and PMB-2 with $M_n = 3880$ kg/mol, $M_w = 6130$ kg/mol, $M_w/M_n = 1.58$ (GPC data).

P2VP of molecular weight ranging from 50 to 800 kg/mol was purchased from Polymer Sources Inc. (synthesized by anionic polymerization, polydispersity index of about 1.1). Random copolymer poly(2-vinylpyridine-*co*-styrene) (P2VP-*co*-PS) (styrene content 30%, $M_w = 220$ kg/mol, $M_n = 130$ kg/mol) was purchased from Aldrich.

Sample Preparation. Solutions of PMB or P2VP (0.0005 mg/mL) were prepared in Millipore water (18 M Om × cm), pH 3 (HCl, Aldrich). A corresponding amount of concentrated salt (NaCl or Na_3PO_4, Aldrich) solution was added, and the mixture was allowed to equilibrate at room temperature for 2 h. The mica was cut and gently pressed onto a sticky tab on a 15-mm diameter metal disk. We then set a drop of the examining solution on the surface of the freshly cleaved mica for 60 s, and afterward we removed the rest of the drop either with centrifugal force or with nitrogen flux. We did not observe any difference in conformations of the visualized single molecules on the samples prepared with these two different procedures. Finally, samples were rinsed with water and dried with nitrogen flux.

Most of the adsorption experiments were done at pH 3 near the isoelectric point (IEP) of mica substrate (see the Supporting Information). The IEP of the freshly cleaved mica was determined by streaming potential measurements with an electrokinetic analyzer (EKA, Anton Paar, Austria). The electric potential was measured as a function of pressure loss in a streaming channel between two mica plates. ζ-Potential was calculated from the streaming potential as described elsewhere.[19] Debye length (λ_D) was calculated as $\lambda_D = (8\pi\lambda_B N_A I)^{-1/2}$, where $\lambda_B \approx 0.7$ nm is the Bjerrum length (an aqueous medium and room temperature), N_A is Avogadro's number, $I = 1/2\sum c_i Z_i^2$ is the ionic strength, and Z_i and c_i are the valence and concentration of ions.

Atomic Force Microscopy. Most of the adsorbed PE molecules are investigated in a dry state with a Multimode AFM instrument (Digital Instruments, Santa Barbara) operating with amplitude feedback in "light" tapping mode (amplitude set point in the range of 0.99−0.95). Silicon tips with a radius of 10−20 nm, spring constant of 0.3 N/m, and resonance frequency of 250−300 kHz were used after the calibration with gold nanoparticles (diameter 5.22 nm, Pelco AFM Gold Standard Kit.) to evaluate the tip radius. Most measurements were done with the tip radius 14.9 ± 1.9 nm. The dimensions of structures obtained from AFM images were corrected (decreased) by the tip radius according to the standard procedure.[20] All measurements were done at ambient conditions (temperature 21 ± 2° C; relative humidity 50−70%). We observed no effect of humidity on the visualized conformations of PE molecules.

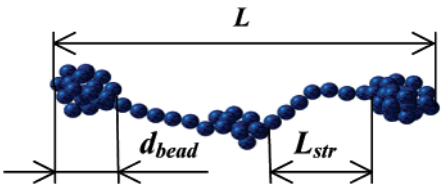

Figure 2. Schematic presentation of pearl necklace globule of the length L, with the diameter of beads d_{bead} and the distance between beads l_{str}.

AFM in Fluid. Freshly cleaved mica was placed into the aqueous solution of PMB-2 (0.0005 mg/mL) with added salt (Na_3PO_4, 8.7 mM; pH 3, HCl) for 1 min and then rinsed in salt aqueous solution with the same salt concentration (Na_3PO_4, 8.7 mM; pH 3, HCl) to remove the excess of unadsorbed PMB-2. Afterward, the mica plate was dried only from the bottom side (the top side was retained wet), gently pressed onto a sticky tab on a 15-mm diameter metal disk, and mounted in the microscope. The measurements were performed in the tapping mode in a sealed fluid cell which was filled with an aqueous solution of Na_3PO_4 (8.7 mM; pH 3, HCl).

Dynamic Light Scattering. The dynamic light-scattering experiments were performed with an ALV5000/E correlator and the light source from the Spectra Physics 125A He−Ne laser operating at 632 nm. The correlator was operated in the autocorrelation mode. The measured intensity correlation functions $g^2(t)$ were analyzed using nonlinear inverse Laplace transformation to obtain the distribution of relaxation times $A(\tau)$, which was recalculated into the distribution of hydrodynamic radius of the scattering particles $A(R_h)$ using the Stokes−Einstein relation $D = kT/6\pi\eta R_h$, where η is viscosity, and T is absolute temperature. The measurements were performed at the concentration regime[21] of PE ($c_p = 0.01$ mg/mL) much below the overlap concentration $c_p^* = 0.46$ mg/mL (for PMB-1). The concentration satisfied the condition for the ratio between the molar PE monomer concentration ($c_p m \approx 4 \times 10^{-4}$ mol/L) and the salt (NaCl) concentration (c_s ranging from 0.004 to 2 M) to be $c_p m/c_s < 0.1$ to avoid the slow diffusive mode occurring in PE solutions and falsifying dynamic light-scattering measurements. All measurements were performed in aqueous solution at pH 2.0 (HCl). At the salt concentration above 0.2 M, we observed on $A(R_h)$ a pronounced peak corresponding to aggregated PE molecules. Above this concentration, we used only the peak which corresponded to the faster diffusive mode, assuming that this peak originates from single molecule globules, but not from their aggregates. Normally, this procedure is not very reliable. Very good agreement between DLS and AFM data supports that such a procedure in this particular case was reasonable.

Results and Discussion

First, we report experiments which suggest that we are dealing with kinetically frozen conformations which reflect the conformations in solution. Second, we show that quantitative parameters characterizing the morphology of single PE chains are consistent with the DRO model. Finally, we discuss the character of CGT.

According to the DRO model, we consider the PE chain (Figure 2) with the f fraction of charged monomers in poor solvent as a necklace globule of the total length L with N_{bead} beads of the size d_{bead} joined by $N_{bead} - 1$ cylindrical strings of the length l_{str}. In our discussion, we associate with L the apparent long axis length measured in a similar way as for stiff DNA molecules as the longest distance in the outline of the polymer

(18) Zimmermann, A.; Jaeger, W.; Reichert, K.-H. *Polym. News* **1997**, 390−392. Jaeger, W.; Paulke, B.-R.; Zimmermann, A.; Lieske, A.; Wendler, U.; Bohrisch, J. *Polym. Prepr.* **1999**, *40*, 980−981.
(19) Jacobash, H.-J.; Simon, F.; Werner, C., Belmann, C. *Tech. Mess.* **1966**, *63*, 447.
(20) Vesenka, J.; Manne, S.; Giberson, R.; Marsh, T.; Henderson, E. *Biophys. J.* **1993**, *65*, 992−997
(21) (a) Förster, S.; Schmidt, M.; Antonietti, M. *J. Phys. Chem.* **1992**, *96*, 4008. (b) Beer, M.; Schmidt, M.; Muthukumar, M. *Macromolecules* **1997**, *30*, 8375−8385.

globule in AFM images.[8] Within an ensemble of molecules, we calculate the number average (L_n) and the weight average (L_w) necklace length. We should distinguish L from contour lengths l of PE chains obtained from the length of a curve line drawn along the contour of the chain backbone. Always L is smaller than l; only in the case of the rodlike chain does $L \approx l$. For convenience, in our discussion, we consider an extended polymer coil and a compact globule as two limiting cases of necklace conformation with dimensions characterized by L. It is clear that L is not a strictly defined parameter for PE in a coil conformation. Therefore, we use L to introduce dimensions of necklace globules, while this value for PE solutions with a small screening effect serves for very rough estimations of molecular dimensions.

What Do We Observe with AFM? Polymer adsorption appears in the literature as a two-step process. The first step is the diffusion-limited adsorption, when the number of adsorbed molecules increases with the square root of time.[22] Chains enter into contact with the surface and adsorb, retaining their solution conformation. The second step is the slow reconformation of the adsorbed chains, when the chains become progressively flatter.[23] Changes occurring during a long period of time of equilibration in adsorbed layers were found to be very slow and have a complicated nonequilibrium character[24] sometime resulting even in oscillation of the adsorbed amount caused by interplay between adsorption, reconformation, and desorption kinetics.[25] Generally, we may expect various possibilities from no change to large changes in the conformation of PE chains after they approach the solid substrate surface. Even in the case of large changes, the reconformation kinetics can be very different. Reconformation characteristic time of the adsorbed chains differs from seconds to hours depending on interactions in the particular system. The polymer molecule can be kinetically trapped by the substrate, and changes in conformation can be detected after a long period of time. This particular case is of special interest for investigations of conformations in solution. In this case, the polymer chain is adsorbed on the substrate surface, retaining its solution conformation, and its two-dimensional (2-D) size correlates with the dimensions of the chain in solvent. If the layer of such deposited molecules is dried, the molecular conformations can be strongly affected by capillary forces and stresses appearing in the trapped chains (due to the local contraction), resulting in buckling and twisting of chains.[26] Nevertheless, for PE, an optimum interaction may provide the case when the 2-D molecular conformation is slightly changed by the contact with substrate and frozen in such a way that during solvent evaporation the polymer coil undergoes the collapse in Z-direction (Z-collapse), while it sustains the collapse in $X-Y$ directions in the plane of the substrate surface. We show below that we found conditions providing this particular case of frozen chain conformations,

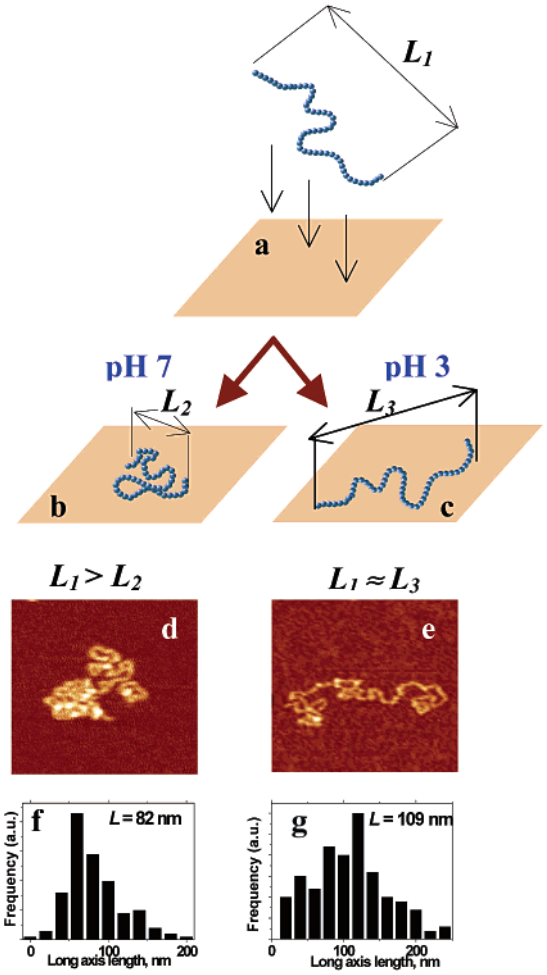

Figure 3. Adsorption of PMB-1 molecules on solid substrate: outline of two possible cases when molecule (a) with the characteristic size L adsorbed and trapped with dramatic change of conformation (b) or with very small change of dimensions (c) and experimental representative AFM images of the conformations on negatively charged (ζ potential -28 mV) (d) and at IEP of mica (e), respectively; histograms showing the differences of the average L after adsorption for both cases (f) and (g), respectively.

when L in solution is very close to this value for PE molecules deposited on mica substrate.

In Figure 3, we outlined the experimental illustration of two different cases of a change of the molecular conformation of PMB-1 chains adsorbed on mica substrate. The PMB-1 chain of characteristic dimension L_1 approaches the mica surface and appears in the dry state as a wormlike coil with the size L_2 or L_3 when adsorbed at pH 3 and pH 7, respectively. Figure 3d and e shows representative AFM images of the adsorbed chains, while in Figure 3f and g we present corresponding histograms obtained from measurements of 150 molecules (from about 15 different images). We may conclude that $L_2 < L_3$, which is in good agreement with the theoretical prediction of adsorption of hydrophobic polyelectrolytes on oppositely charged surfaces.[27] At pH 3, the mica surface is only slightly negatively charged, while a much larger negative charge at pH 7 enhances screening of the intrachain Coulombic repulsion in PMB-1, which appears in the more coiled conformation. Most of our following experiments we performed near the IEP of mica at a

(22) See, for example: Motschmann, H.; Stamm, M.; Toprakcioglu, C. *Macromolecules* **1991**, *24*, 3681.
(23) Franz, P.; Granick, S. *Phys. Rev. Lett.* **1991**, *66*, 899.
(24) Pefferekorn, E.; Carroy, R.; Varoqui, R. *J. Polym. Sci., Polym. Phys. Ed.* **1985**, *23*, 1997. Pefferkorn, E.; Haouam, A.; Varoqui, R. *Macromolecules* **1989**, *22*, 2667. Johnson, H. E.; Granick, S. *Macromolecules* **1990**, *23*, 3367. Johnson, H. E.; Granick, S. *Science* **1992**, *255*, 966.
(25) Voronov, A.; Pefferkorn, E.; Minko, S. *Macromol. Rapid Commun.* **1999**, *20*, 85−87. Minko, S.; Voronov, A.; Pefferkorn, E. *Langmuir* **2000**, *16*, 7876−7878.
(26) Sheiko, S. S.; Möller, M. *Chem. Rev.* **2001**, *101*, 4099−4123.
(27) Borisov, O. V.; Hake, F.; Vilgis, T. A.; Joanny, J.-F., Johner, A. *Eur. Phys. J. E* **2001**, *6*, 37−47.

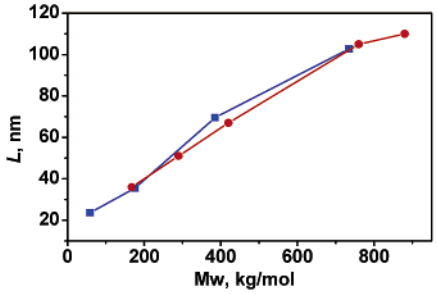

Figure 4. Comparison of the molecular weight dependence of L obtained from AFM data (circles) and $L = k_1 \times R_g$ ($k_1 = 2.2$), where R_g was used from static light-scattering data (published by M. Beer, M. Schmidt, and M. Muthukumar[21b]) (squares) for protonated P2VP.

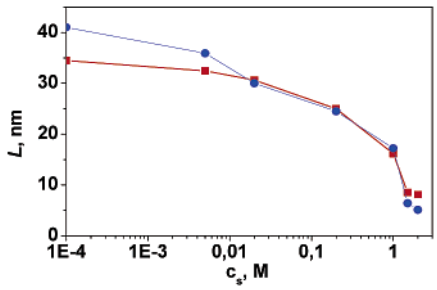

Figure 5. Comparison of the ionic strength dependence of L obtained from AFM data (squares) with $L = k_2 \times R_h$ ($k_2 = 3.0$), where R_h is the hydrodynamic radius for PMP-1 in NaCl solutions obtained from DLS (circles) experiments.

pH ranging from 2 to 3, assuming that in this case the surface introduces minimal changes in PE molecular conformations.

Now we can address the question of how far is L_3 from L_1? We found very good correlation between these two values comparing results of light-scattering experiments with AFM data for PE molecules of different length and for different ionic strengths of PE solutions (Figures 4 and 5). In Figure 4, we compare L values obtained from AFM images for P2VP adsorbed on mica at pH 2 (HCl 0.01 M) with the published elsewhere[21b] values of gyration radius (R_g) of protonated P2VP (HBr 0.01 M) of different molecular weights. We use an empirical relationship $L \approx k_1 \times R_g$, where $k_1 = 2.2$ is a fitting coefficient. In Figure 5, we compare L with the dynamic light-scattering hydrodynamic radius (R_h) taking $L \approx k_2 \times R_h$, where $k_2 = 3.0$, for PMB-1 molecules at different ionic strengths of PE solutions. In these calculations, the histograms for L (available from the Supporting Information) were fitted to a normal distribution to obtain the mean value. Both series of experimental data clearly show the good agreement between molecular dimensions in solution and deposited on mica substrate at IEP. Consequently, the molecular conformation is not substantially changed during adsorption and following drying, and we may take that $L_1 \approx L_3$.

The following experiment additionally proves that the adsorbed PE chains are kinetically trapped on the surface and the molecular conformations are frozen. The mica plate was dipped in the aqueous solution of PMB-2 for 2 min. Afterward, we replaced with the help of a syringe the PE solution with water and then with acetone, or aqueous acetone (90%), or a concentrated (18 mM) solution of Na_3PO_4. In all cases, we compared conformations of the adsorbed PE molecules (reference) (Figure 6a,c) with those after the treatment with the condensation agents (Figure 6b,d).

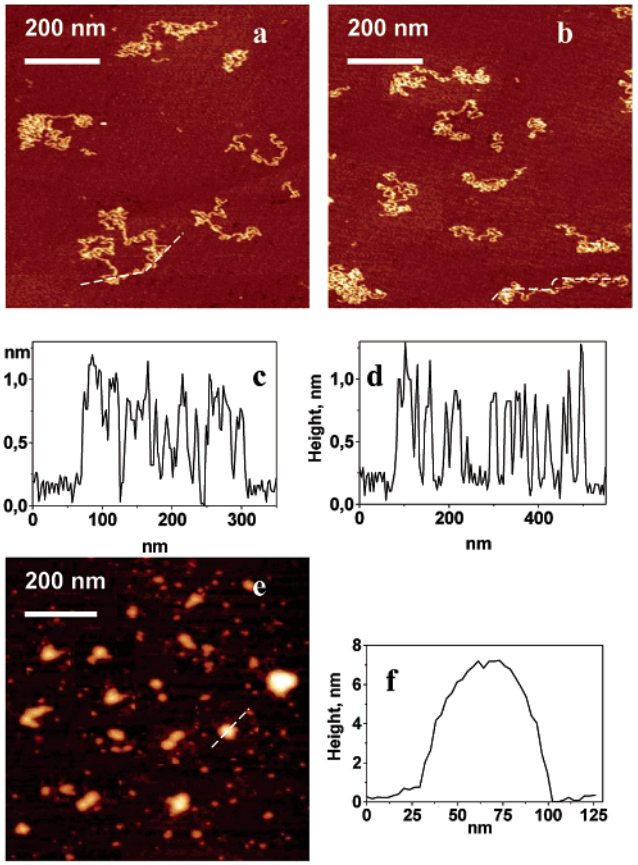

Figure 6. AFM images (800 × 800 nm^2) of PMB-2 single molecules deposited onto mica: in extended conformations (Z-range 2 nm) from pH 3 aqueous solution and dried (a); similar experiment, but after deposition the wet sample was introduced into acetone for 5 min and dried (Z-range 2 nm); because of the strong interaction with the substrate, no change was detected in 5 min of exposure (b); in globular conformation from solution in 9:1 acetone:water (pH 3) mixture. (c), (d), (f) − cross sections from (a), (b), (e), respectively.

We found no changes in molecular conformations. The second reference sample (Figure 6e,f) presents the globular molecular conformation of PMB-2 prepared directly from 90% acetone aqueous solution. Comparing these data, we may conclude that adsorbed conformations of PE molecules are very far from equilibrium and they are frozen by the strong nonelectrostatic interaction with mica. It is unlikely for this case that morphology of the adsorbed molecules can be changed during drying in this system. When we dry the sample, mainly Z-collapse is observed. We repeated the same procedure when we initially deposited PE molecules in necklace-globule conformations, and then before drying we treated the samples with condensation agents. The experiments had the same results: no changes in the frozen necklace conformations were observed with AFM. We should mention that exposure of the samples to solutions for much longer periods of time (tens of hours) results in a change of the molecular conformation and equilibration of the conformations of the adsorbed molecules. We plan to report the latter results in our future publication.

Additional facts also support our conclusions about frozen conformations. We found no effect of humidity on the molecular conformations. Even ion exchange of adsorbed PMB with polyvalent ions effected no large change in molecular conformations. That allowed us to overcome the $X-Y$ collapse and metallize the single molecules in different conformations.[3]

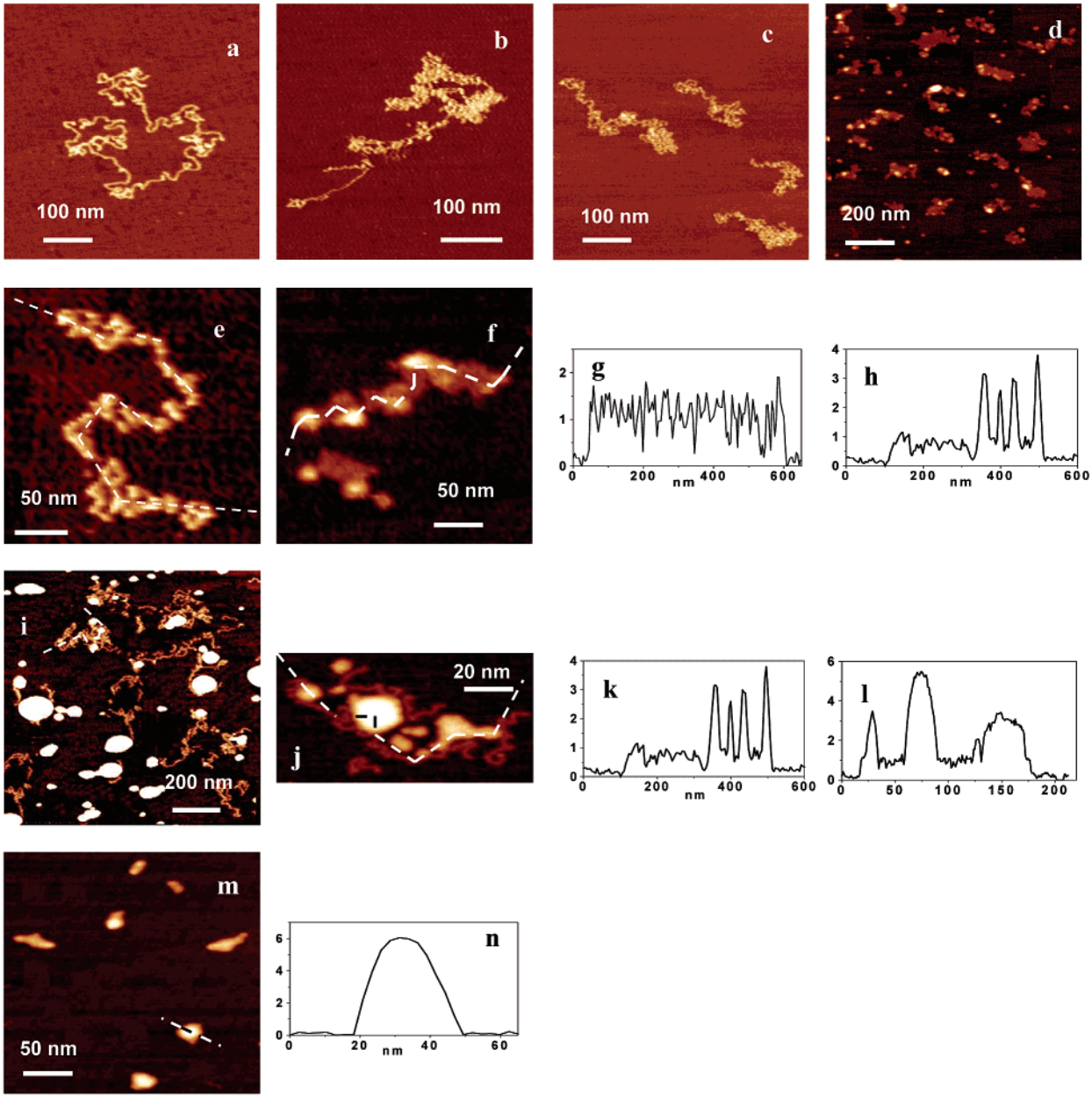

Figure 7. AFM images of PMB-2 single molecules deposited from aqueous solutions: reference, no salt (a) and with added Na_3PO_4: 4.2 mM (b); 6 mM (c and e); 8.4 mM (d and f); 8.7 mM (i); 12 mM (j); 18 M (m). Cross sections from AFM images: (g) corresponds to (e); (h) corresponds to (f); (k) corresponds to (i); (l) corresponds to (j); (n) corresponds to (m). We present the cross section from original (no deconvolution) AFM images. The dimensions corrected by the tip radius are presented in Figure 8 and in Table 2.

Cascade of Necklace-Globule Transitions. In Figure 7, we present the series of experiments when we study the stepwise CGT of PMB-2 molecules in aqueous solutions by adding Na_3PO_4. Similar experimental data for PMB-1 molecules with added NaCl are available as Supporting Information. In salt-free solutions, both polymers appear as extended coils (Figure 7a). Dimensions of the PE molecules such as number average (l_n) and weight average (l_w) contour length, polydispersity index (PDP $= l_w/l_n$), height, and width obtained from the statistical analysis of 150 structures on 18 AFM images are presented in Table 1.

We were not able to measure the contour length of PMB-2 molecules because they appeared in more coiled conformations, and we met the problem to identify the ends of the coils. These results suggest that we observe a 2-D projection of the elongated coil due to the Coulomb repulsion PE coils. No signs of $X-Y$ collapse during sample preparation were found on AFM images. The height of the structures is consistent with the size of the monomer.

Table 1. Average Sizes of PMB Molecules As Appeared in AFM Images

PE	contour length, nm l_n/l_w/PDI	height, nm	width, nm
PMB-1	319/454/1.42	0.75 ± 0.15	2.4 ± 0.6
PMB-2		0.72 ± 0.18	2.3 ± 0.8

Added salt dramatically changes molecular conformations and the fine morphology of PE chains. Images in Figure 7b−n clearly show intramolecular segregated areas. Two pronounced differences from salt-free solution can be found on the images:

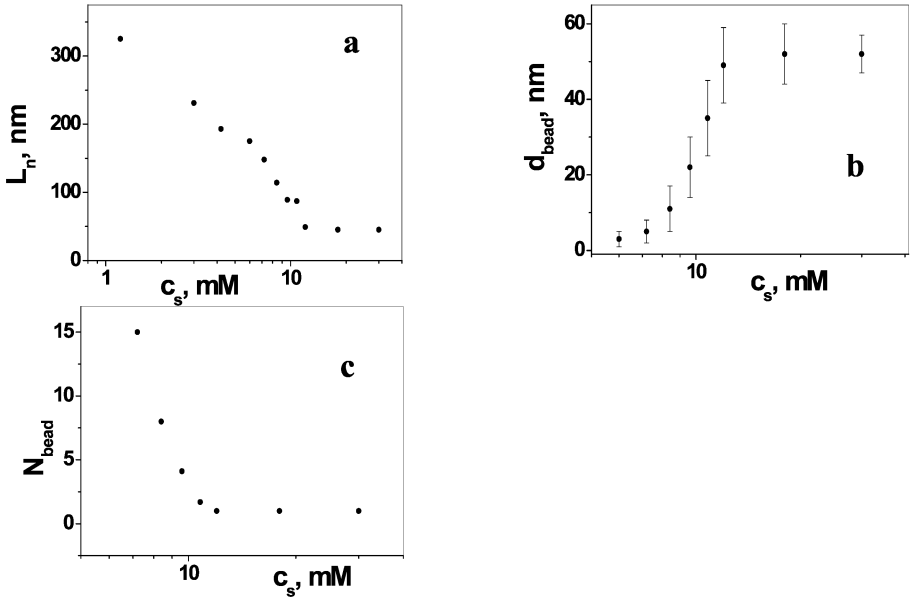

Figure 8. Ionic strength dependence of average quantitative characteristics of pearl necklaces: length on necklace globule (a); diameter of beads (b); number of beads per globule (c).

the polymer coil starts to segregate into small beads nicely observed in the zoom image in Figure 7e,g; the beads segregate in big clusters. The height of the beads is several times larger than the height of the backbone. We assume according to the DRO model that the beads are formed due to the PE intrachain segregation induced by the screening effect of the added salt and due to the enhanced attraction induced by condensed salt ions, while larger clusters are apparent structures resulting from the deposition (projection) of PE globules on the substrate. The latter can be understood if we compare Figure 7a and c. Molecules deposited from salt-free solution appear in the 2-D projection as a sequence of connected highly coiled areas due to thermal fluctuations and a free rotation of the chain in solution when a particular conformation and orientation of the molecule with respect to the plane of solid substrate is suddenly frozen due to the adsorption. It is necessary to mention that, despite diversity of possible orientations of PE globule in solution with respect to the plane of substrate, they adsorb in such a way that long axis length of the globule is always oriented almost parallel to the substrate because we always have $L_1 \approx L_3$.

The intrinsic beads and apparent cluster of beads can be distinguished due to the alternating thickness of the structures on the cross section of the images (Figure 7g, h, k, l, and m). Clusters of the beads have a very rough surface formed by a closely packed sequence of beds, while beads appear on the cross section as smooth bumps. Each step of adding salt results in the increase of the size of beads and the decrease of their number, as well as the decrease of the necklace length as it is shown in Figure 8.

Additionally, the characteristics of molecular dimensions are presented in Table 2. These results are in good qualitative agreement with the DRO theory, which suggests the effect of charge density f on chains: $L \propto f$; $d_{bead} \propto f^{(-2/3)}$; $N_{bead} \propto f^2$. In our experiments, we increase the ionic strength of the solutions which show similar charge density but inverse influence on PE molecular conformations due to the screening of the Coulomb interaction and due to the enhanced attraction induced by condensed salt ions. We cannot calculate l_{str} directly from AFM images. The evaluation of this value as $l_{str} = (L - N_{bead}d_{bead})/(N_{bead} - 1)$ results in a large error; nevertheless, it shows that changes in globule conformations occur at $\lambda_D \leq l_{str}$. Therefore, the local conformation of the necklace is perturbed when the screening length becomes comparable to the distance between beads. In the range of the ionic strength of the solutions, the screening length changes by only a factor of 2. Consequently, the observed dramatic conformation change of the necklace globules is mainly effected by the enhanced attraction introduced by added counterions. It is remarkable that at an ionic strength larger than 6 mM, we observe a sharp transition of necklaces to dumbbell conformations or a single globule with loops and tails (Figure 7i and j). Also, we explain this abrupt transition by the contribution of the ion condensation effect. The increase of the necklace density with the increase of ionic strength promotes the ion condensation.[15] This effect leads to counterion-induced attraction between different parts of the chain, and, because of a feedback-type mechanism, it amplifies the collapse.[28] This mechanism can be enhanced by polyvalent ions

Table 2. Molecular Dimensions of PMB-2 Globules Deposited on Mica from Na_3PO_4 Solutions at pH 3

ionic strength, M	Debye length, λ_D, nm	size of necklace L_w/L_n/PDI (L_w and $L_n \pm 10$ nm)	average diameter of beads, d_{bead}, nm	average number of beads, N_{bead}	distance between beads, $l_{str} \pm 3$ nm	average height of structure, nm
0	9.7	334/248/1.34				0.8 ± 0.2
0.007	3.4	325/201/1.61				0.8 ± 0.2
0.018	2.2	231/177/1.42				0.8 ± 0.2
0.025	1.9	193/163/1.19				0.8 ± 0.2
0.036	1.6	175/140/1.25	3 ± 2	28 ± 10	3	0.8 ± 0.2
0.043	1.5	148/103/1.44	5 ± 3	15 ± 5	5	1.2 ± 0.3
0.050	1.4	114/99/1.16	11 ± 6	8 ± 3	3	2.5 ± 0.5
0.058	1.3	89/65/1.37	22 ± 8	4 ± 2	0.3	4.1 ± 0.8
0.065	1.2	87/56/1.56	35 ± 10	2 ± 1		4.9 ± 1
0.072	1.1	49/61/1.25	49 ± 10	1		5.5 ± 1
0.108	0.9	45/51/1.14	45 ± 8	1		5.5 ± 1
0.180	0.72	45/55/1.21	45 ± 5	1		5.5 ± 1

(28) Schiessel, H.; Pincus, P. *Macromolecules* **1998**, *31*, 7953−7959.

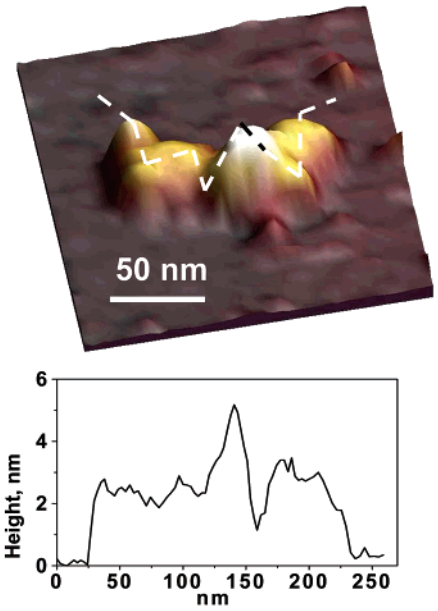

Figure 9. AFM image of PMB-2 under aqueous solution with added 8.4 mM of Na_3PO_4.

in the case of Na_3PO_4. It is noteworthy that the formation of the globule conformation by PMB-1 molecules in NaCl solution was observed at an ionic strength 30 times larger than that for the case of Na_3PO_4 solution.

Finally, we prove that the observed necklace structures are not introduced by drying of the samples. In Figure 9, we present the AFM image of the necklace morphology obtained by scanning under aqueous solution. Despite a poorer resolution, the intramolecular segregated beads are clearly pronounced on the image and the cross section.

We studied the sample of P2VP-*co*-PS to demonstrate the role of hydrophobic interactions in the formation of the intramolecular segregated structures. As we demonstrated in our previous publication,[17] P2VP adopts an extended coil conformation in aqueous solution at pH 2, and necklaces are formed with an increase of pH values. Figure 10 indicates that the P2VP-*co*-PS copolymer shows the necklacelike morphology at pH 2. In this copolymer, the balance between hydrophobic and Coulomb interactions is shifted due to the introduction of styrene monomers.

Character of CGT. The plots of molecular dimensions versus ionic strength (Figure 8) show the narrow but continuous CGT region. At the same time, we identified on AFM images the coexistence of extended coils, and necklacelike and compact globules with loops and tails of nonsegregated segments (Figure 7i and j). Such a coexistence is considered as a sign of the first-order phase transition. This picture is very similar to those observed for the first-order transition of rigid DNA molecules when the discontinuous process on the level of single molecules appears as a continuous transition within a finite assemble of molecules.[8] This result is a very nice example demonstrating similarity in nature. In the case of flexible hydrophobic PE, the superposition of the first-order transitions between necklaces with different amount of beads results in the apparent smooth character of the process for the assembly of PE molecules. As it was mentioned above, the ion condensation mechanism can even enhance the sharp transition.

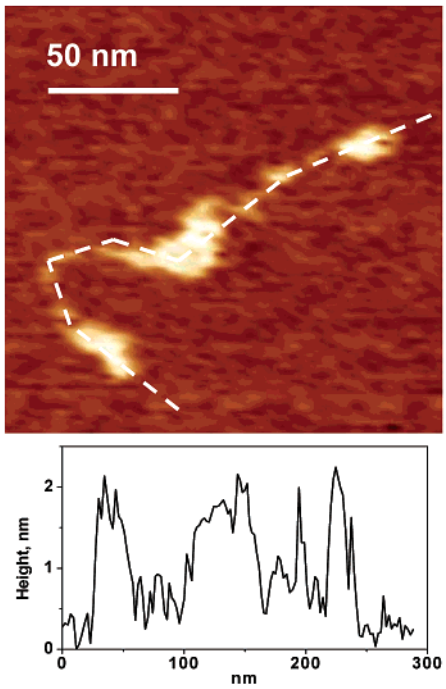

Figure 10. AFM image of P2VP-*co*-PS single molecules deposited from aqueous solution at pH 2.

Histograms of size distribution (available in the Supporting Information) also indicate the coexistence of coil and globule conformations in each step of the transition, although the bimodal character of the histograms is not always very well pronounced because of the superposition of the cascade of CGT.

Therefore, PE molecules occupy an intermediate place between stiff chains collapsing by the first-order-type phase transition and flexible polymers collapsing by the second-order-type phase transition. This intermediate place is caused by the abrupt splitting of the PE globule into charged beads when the necklace globule jumps from one to another conformation with different amounts of collapsed beads as effective repulsion decreases.

Conclusions

P2VP and PMB PE molecules are kinetically trapped on mica surface at the isoelectric point and undergo *Z*-collapse during drying of the sample, while in the $X-Y$ direction the conformation is only slightly changed. The molecules appear as elongated coils or pearl necklacelike globules depending on the ionic strength of the solution. The size of the deposited single molecules correlates very well with molecular dimensions in solution obtained in light-scattering experiments.

The increase of the ionic strength of solution of these flexible hydrophobic PE results in CGT between the extended coil and compact globule conformations through the cascade of intermediate necklacelike globules with a decreasing amount of beads. The size of the beads increases with an increase of the ionic strength. The coexistence of extended coils, necklacelike globules, and compact globules indicates the cascade of the first-order CGT.

Acknowledgment. The authors thank Dr. C. Bellmann, Mrs. N. Petong, and Dr. C. Froeck for their help and assistance. We thank Dr. E. Pefferkorn for the fruitful discussion. We are

grateful for the financial support provided by the DFG priority program "Polyelektrolyte" and NATO Linkage Grant EST-CLG 976188.

Supporting Information Available: Histograms representing distribution of the length of necklaces of PMB-2 deposited on mica from aqueous solutions at pH 3 and different concentrations of Na_3PO_4; AFM images of PMB-1 molecules deposited on mica from aqueous solutions at pH 3 with added NaCl; histograms representing distribution of the length of necklaces of PMB-1 deposited on mica from aqueous solutions at pH 3 and different concentrations of NaCl; ζ-potential of mica surface versus pH at 0.001 M KCl aqueous solution (PDF). This material is available free of charge via the Internet at http://pubs.acs.org.

JA0261168